**Proceedings Paper:**
Adugu, AK and Tsavdaridis, KD (2019) Eurocode 9 Cross-Section Classification of Optimised Aluminium Profiles in Compression. In: Lam, D, Dai, X, Sheehan, T, Yang, J and Zhou, K, (eds.) Proceedings of the 9th International Conference on Steel and Aluminium Structures ICSAS19. The 9th International Conference on Steel and Aluminium Structures., 03-05 Jul 2019, Bradford, UK. Independent Publishing Network, pp. 152-163. ISBN: 978-1-78972-197-3. ISSN: 0141-0296.

This is an author produced version of a paper published in Proceedings of the 9th International Conference on Steel and Aluminium Structures (ICSAS19).

9th International Conference on
Steel and Aluminium Structures (ICSAS19)
Bradford, UK, 3-5, July, 2019

# EUROCODE 9 CROSS-SECTION CLASSIFICATION OF OPTIMISED ALUMINIUM PROFILES IN COMPRESSION

**Alikem Kobla ADUGU[a] and Konstantinos Daniel TSAVDARIDIS[b]**

[a] Engineer, WSP, 3 White Rose Office Park, Millshaw Park Lane, Leeds, LS11 0DL, UK
Email: alikemadugu@gmail.com

[b] Associate Professor of Structural Engineering, School of Civil Engineering, University of Leeds, Leeds, LS2 9JT, UK
Email: k.tsavdaridis@leeds.ac.uk

**Keywords**: Cross-section classification, Eurocode 9, Structural Topology Optimisation, Manufacturability criteria, Aluminium profiles, Stub-column tests

**Abstract**. *Aluminium alloys are widely used due to their advantageous properties, i.e., their light-weight, high corrosion resistance, and high recyclability. A disadvantage of using aluminium alloys is their low elastic modulus which is almost three times less than that of the steel. To use aluminium alloys more often in structural applications, the stiffness of such structural elements (stiffness-to-weight ratio) has to be increased. To achieve this, structural topology optimisation (STO) can be employed as it can produce the optimum distribution of the material in the cross-sectional domain. This paper focuses on a recently optimised aluminium section and further improves its manufacturability by creating new profile shapes with a combination of both straight and curved elements. Stub-column tests were conducted through finite element (FE) analyses to determine the behaviour of the optimised aluminium sections under compression and investigate the effectiveness of using existing methods for their classification. It was found that Eurocode 9 can be used for the classification of these novel aluminium profiles.*

## 1 INTRODUCTION TO ALUMINIUM

### 1.1 Advantages and Disadvantages

Aluminium makes up about 8% of the earth's crust making it the most abundant metal within this layer [1]. Aluminium alloys are used in a variety of applications in aerospace and in the automotive industry. This is due to its favourable properties such as its low density, high malleability, high corrosion resistance, and high recyclability [2]. For a plethora of structural applications, members with minimal weight and increased strength are required. This search for structural elements with a high weight-to-stiffness ratio can potentially be met by aluminium. Aluminium alloys are suitable to fit the desired weight-to-stiffness ratio due to their lightweight nature. However, the low elastic modulus (E) of aluminium alloys may yield undesirable results, for instance, members prone to local instability and buckling.

Aluminium is mainly manufactured by the extrusion process, which is beneficial in terms of the diversity of cross-sectional shapes that can be produced. Along with that, new manufacturing techniques such as 3D printing, which can create any complex in geometry sections with varying cross-sectional area distributions, can be effectively adopted when using aluminium alloys. The development of cross-sectional shapes that yield stiffer structural

elements than the current ones is in demand nowadays and this is examined with the use of advanced computational structural topology optimisation tools.

Researchers have used structural optimisation to modify existing sections [3,4,5,6] but there is no evidence of using structural topology optimisation (STO) for developing new aluminium profiles. Tsavdaridis et al. [7,8] have exploited the use of STO for the development of new cross-sectional shapes and compared them to a few existing standard aluminium profiles. Similar comparisons of these novel shapes to existing sections [9,10,11,12] have been established and it was concluded that the novel shapes are competitive in performance. The aim of this follow-up complimentary paper is to characterise their sectional behaviour towards the development of design guidelines.

### 1.2 Manufacturing Aluminium

To produce aluminium, it must be obtained in its mineral form, bauxite, which contains aluminium oxide. Aluminium is then extracted from bauxite via electrolysis. The pure aluminium is then combined with another element to produce an alloyed metal [13]. The metal is then turned into ingots, sheets or extrusions. For structural bearing uses, the next stage is usually *extrusion*.

During the extrusion process, the hot metal (aluminium billet) is forced through an opening with a specific cross-sectional shape, aka the die. The final aluminium cross-section matches the die profile; thus *complex* shapes can be produced using this process [14]. Consequently, engineers have the flexibility to produce a large variety of complex cross-section shapes to meet the structural requirements.

### 1.3 Aluminium as Structural Material

The use of aluminium as a structural material has risen in frequency over the last few decades. Aluminium alloys have been used widely in the aeronautical industry and in other branches of transport such as in railways, cars and shipping [1].

Structural building applications of aluminium are mainly non-structural, in the form of secondary elements such as roofing, curtain walls, window frames, facades, and door frames. The widespread use in these fields comes from its low density, high corrosion resistance and high recyclability [15].

Such properties make aluminium a strong candidate for use as a primary load bearing element [16]. The low elastic modulus has an impact on its bending stiffness (EI), which is directly proportional to the stability of the structural element, thus influences beam deflection and the likelihood of buckling. However, a cross-section which uses the same cross-sectional area whilst increasing the moment of inertia can tackle the low stiffness issue. Structural topology optimisation provides a targeted process for the development of structurally efficient cross-sections to effectively resist a combination of loads with minimal use of material [17].

## 2 STRUCTURAL OPTIMISATION

### 2. 1 Structural Topology Optimisation

Structural topology optimisation (STO) can be split into two groups; the material/microstructure approach and the geometrical/macrostructure approach [18]. The microstructure approach is described by Holmberg et al. [19] as a method which obtains the optimal structural topology by varying the material density within a restricted grid or domain.

An example of the microstructure approach is the Solid Isotropic Material with Penalisation (SIMP) technique developed by Bendsøe [20]. This method uses a penalisation

factor to suppress the intermediate densities thus resulting in a solution where each element has a density of 0 or 1 (i.e., each element is either on or off; black or white).

The macrostructure approach differs from the microstructure approach in that the starting point of the macrostructure approach is a domain/grid filled with material. The material is then removed from areas within the domain which are underutilised during the optimisation process. Another difference is that the finite element mesh (i.e., the shape and number of elements) changes as well as the amount of material used. An example of the macrostructure approach is the Evolutionary Structural Optimisation (ESO) technique developed by Xie and Steven [21]. A comparison of the SIMP and ESO techniques undertaken by Rozvany [22] showed that SIMP is the most popular STO technique used in many industries in multiple commercial FE analysis software and this is mainly because the SIMP technique does not require initial inputs of specific member sizes and dimensions, thus the designer does not need to have a notion of the final result [22].

### 2.2 Previously Optimised Aluminium Profiles

STO has been used in order to create optimised beams and columns [4,15,23,24,25]. In Grekavicius et al. [7], the complimentary STO study, the sections optimised using the SIMP technique with minimum weight design. In specific, beam and column loading conditions were simulated to develop novel cross-sectional morphologies. Around 40 loading conditions were examined, such loading conditions that the structural elements of modular units may experience. The optimisation was performed on square and rectangular domains and it was concluded that the effect is the same, therefore more efforts were concentrated using the square domain.

Ten novel cross-sections were developed and tested by Grekavicius et al. [7]. This paper deals with one of the best performing sections (Figure 1).

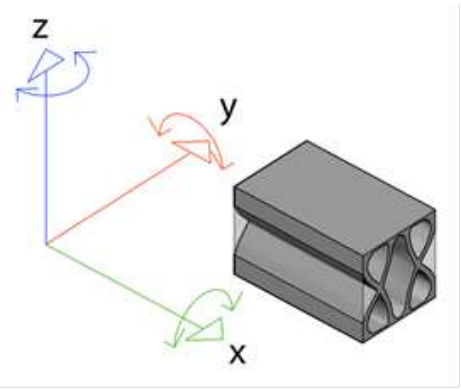


Figure 1: Image of the optimised section to be used in these calculations [7].

## 3 NUMERICAL MODELLING

FEA software Abaqus/CAE 2017 was employed to model the elasto-plastic behaviour of aluminium through a stub column test in order to understand the local buckling behaviour due to axial compression forces of the newly optimised cross-section.

## 3.1 FEA Parameters

### 3.1.1 Material Properties

The same materials as in the complimentary paper are chosen herein to remain consistent with the previous FE analyses [7], thus the properties of aluminium alloy 6063-T6 are adopted.

Due to large variations in the types and properties of aluminium alloys, Eurocode 9 (EC9) [26] Annex E suggests the best way to calibrate the properties of any aluminium alloy is via a tensile test. Due to limited resources, this method was not used in this investigation. Instead, the nominal values found in EC9 were entered. Annex E of EC9 allows for the modelling of aluminium plastic behaviour using linear models. This annex allows for a bi-linear relationship.

Residual stresses are usually insignificant for extruded sections [1] and their use in FE modelling has demonstrated to have little influence as reported by Liu et al. [27], thus residual stresses were not included in this study.

The most critical failure mode was the first eigenmode of the eigenvalue buckling analysis stage, as it required the lowest magnitude of force. This agrees with Tsavdaridis and D'Mello [28] and the first eigenmode with a specific scale of imperfection best reflects real-life behaviour. For extruded profiles, national specifications allow for a thickness deviation of 5% but this increases to 10% when thicknesses are less than 5mm. Thus, 0.5mm is the worst-case value, and so the magnitude of geometrical imperfection used.

### 3.1.2 Boundary conditions and loading

Stub column tests can be done with a pin-ended or fixed-ended column (Figure 2). The fixed-ended arrangement is considered best for investigating cross-sectional instability or local buckling. Mennink [29] noted that this is because in pin-ended columns, the centre of gravity of section shifts during the test resulting in an eccentricity in the applied load which induces a bending moment within the section.

To mimic a fixed-end stub column test, rigid plates were used. These rigid plates simulated the interaction between the test machine and the column ends. One of the rigid plates is fixed and the other one is free to move axially towards the column thus applying the compressive force required. The column ends are constrained by the boundary conditions applied to the Reference Point (RP) at the centroid of the section. To model the fixed rigid plate, the 'encastre' condition was used with all degrees of freedom constrained. To model the movable rigid plate, all lateral displacements except the Z-axial displacement were constrained.

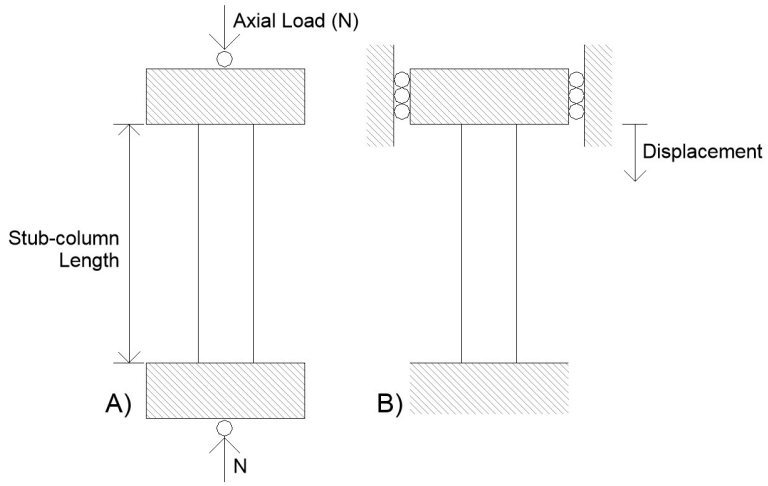


Figure 2: Stub-column test setup. A) Pinned-end B) Fixed-end. Modified from Mennink [29].

3.1.3 Mesh study and model validation

The irregular shape of the novel cross-sections makes the use of a regular mapped mesh impractical and erroneous. Instead, a free mesh using triangular elements was able to achieve accurate results. The mesh sensitivity analysis and model validation were done simultaneously by comparing results from FE models with varying mesh sizes to experimental results from the literature.

The experimental model used for validation was the H70 x 55 x 4.2C-R section from Su et al. [30]. The FE model and experimental test results were compared using the following criteria: maximum load obtained, load-axial displacement curve, and failure deformation shape. Table 1 shows a summary of the validation test results.

The maximum loads obtained from the FE analysis ($P_{FEA}$) are within 5-10% of the experimental result ($P_{Test}$ = 196.9kN) from Su et al. [30] as shown in Table 1. There is also a significant increase in the computational time due to the reduction in mesh size, thus a 5mm mesh size is adopted.

Table 1: Mesh sensitivity analysis results

| Mesh size | Element Numbers | Node Numbers | CPU Time | $P_{FEA}$ (kN) | $P_{Test}/P_{FEA}$ |
|---|---|---|---|---|---|
| 4mm | 38,121 | 62,275 | 44 mins | 186.9 | 1.05 |
| 5mm | 19,222 | 32,672 | 20 mins | 186.4 | 1.06 |
| 6mm | 12,036 | 20,806 | 7 mins | 184.1 | 1.07 |
| 8mm | 7,906 | 13,448 | 3 mins | 180.5 | 1.09 |

# 4 MANUFACTURABILITY ADVANCES VIA HEURISTIC METHODS

## 4.1 Introduction

Before undertaking the full parametric analysis to characterise the sectional behaviour under compression, the manufacturability one of the optimised sections previously proposed is aimed to be improved. Improving the cross-section manufacturability was found necessary to meet the requirements for extrusion, thus allowing for possible fabrication of the novel cross-section.

The rules that are used to improve the manufacturability of the section are the following:

- Retain the maximum thickness ratio across the sections to 2:1 in order to fit within current extrusion limits
- The new designs should have a similar cross-sectional area and should perform similarly (i.e., within ±5%) to the original optimised section under the following criteria: moment of inertia, radius of gyration and local elastic buckling load.

Using the above rules, a plethora of profiles can be developed. This work focuses on the modification of one of the best performing optimised sections as previously proposed by Grekavicius et al. [7]. The configuration of the square profile shows five separate voids (one central elliptically-based void surrounded by four other voids). The principle concept was preserved throughout the creation of the manufacturing shape options. The parameters varied were the size and shape of the voids. A heuristic morphogenesis process further refined the topologically optimised profile. Cross-sectional properties such as the second moment of area, radius of gyration, and the theoretical section compressive buckling load were measured.

A variety of alternative designs (options) were examined based on the use of straight and curved elements. The corners kept at 90º angles, as this is the norm for extruded aluminium sections. Variations in the potential sections come from the use of vertical or inclined (sloppy) web elements. Under these restrictions, four potential forms (options) have been developed (Figure 4).

One of the forms (Option 1) closely mimics geometrically the previously developed beam optimised section. The section is based on the idea that the original shape can be simplified as two flanges stiffened using two 'X' elements; the evolution of this profile is shown in Figure 3. The variation between the sections generated by changing the angle of the internal web element. Table 2 summarises a comparison between the initial optimised section, and the new - better in terms of fabrication - options. In Table 2, the values in brackets show the percentage difference between the original value and the option being considered.

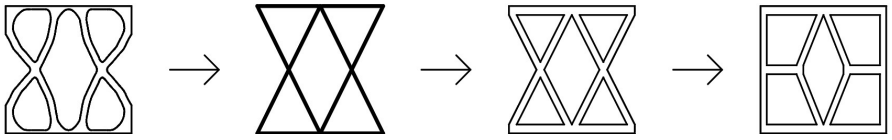

Figure 3: Evolution of Option 1 developed by Grekavicius et al. [7]

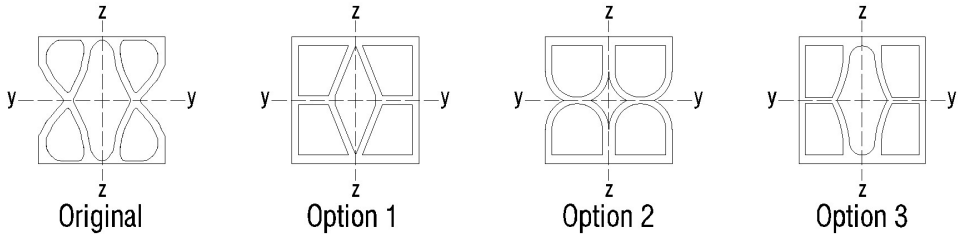


Figure 4: Final cross-section options to be considered

Table 2: Cross-sectional properties of new options compared to original optimised profile

| Properties | Original | Option 1 | Option 2 | Option 3 | Option 4 |
|---|---|---|---|---|---|
| Area [$cm^2$] | 35.0 | 34.4 (-1.7%) | 34.1 (-2.6%) | 35.0 (0%) | 35.3 (+0.9%) |
| Moment of inertia, y [$cm^4$] | 380 | 434 (+14.2%) | 429 (+12.9%) | 413 (+8.7%) | 395 (+3.9%) |
| Moment of inertia, z [$cm^4$] | 319 | 298 (-6.6%) | 392 (+22.9%) | 363 (+13.8%) | 354 (+11.0%) |
| Radius of gyration, y [cm] | 3.29 | 3.55 (+7.9%) | 3.55 (+7.9%) | 3.43 (+4.3%) | 3.34 (+1.5%) |
| Radius of gyration, z [cm] | 3.02 | 2.79 (-7.6%) | 3.39 (+12.3%) | 3.21 (+6.3%) | 3.16 (+4.6%) |
| Local buckling load [kN] | 1350 | 1289 (-4.5%) | 785 (-41.9%) | 1310 (-3.0%) | 1078 (-20.1%) |

### 4.2 Options' Comparison

According to Table 2, all new cross-sections produced have higher sectional properties than the original shape with respect to the second moment of area and radius of gyration. This demonstrates that the heuristic shape optimisation used was successful in terms of meeting both the performance and manufacturing criteria.

The following analysis is done using information from Table 2. Any references to the major and minor axes are the y-y and z-z axes, respectively. Option 1 provides the highest moment of inertia and the highest radius of gyration in the major axis. However, Option 1 has the lowest moment of inertia and the lowest radius of gyration in the weak axis. Consequently, the section shape mainly uses its area to effectively provide stiffness in the major axis but due to the ineffective area use in the minor axis, the section may be susceptible to global buckling in the weak axis. Additionally, Option 1 has the lowest compressive buckling load due to the internal web elements are slenderer, thus more susceptible to buckling.

Option 2 performs alike Option 1 in the major axis, but it provides a higher moment of inertia and radius of gyration in the minor axis. Hence, Option 2 utilises its area more effectively to provide cross-sectional stiffness in both the major and minor axis. Option 3 provides a higher moment of inertia and radius of gyration in both the major and minor axes than Option 4. Option 3 also provides a lower local buckling load. Option 3 is preferred to Option 4 due to the higher radius of gyration in both the major and minor axes.

Option 3 provides nearly double the buckling capacity of Option 2 but Option 3 provides a smaller radius of gyration in both the weak and major axes than Option 2. Option 3 is preferred to Option 2 due to the significantly higher buckling capacity. Option 3 provides a smaller major axis radius of gyration than Option 1, but it provides a higher buckling load than Option 1 and a higher radius of gyration in the weak axis. Consequently, Option 3 will be chosen as the best of the manufacturable sections developed in this investigation.

## 5 CHARACTERISATION OF CROSS-SECTIONAL BEHAVIOUR

The design of the members comes under the broad element behaviours of compression, tension, shear, flexure (bending), and torsion. EC9 provides guidance as to how these checks can be done for standard aluminium cross-sections. This paper focuses on the cross-sectional behaviour under compression.

### 5.1 Cross-section Classification

EC9 deals with the cross-section classification of aluminium members in a similar fashion to that of steel members in Eurocode 3 [31], based on the work of Mazzolani [16]. EC9 places cross-sections into four behavioural classes. These classes describe the global behaviour of sections (i.e., under compression, flexure, or shear). According to EC9, cross-section classes are defined by the capability of the section to reach four defined limit states which are: elastic buckling limit state, elastic limit state, plastic limit state, and collapse limit state.

EC9 classification depends on the material proof strength, the slenderness of the individual compression parts (i.e., width-to-thickness ratios of webs and flanges), the use of welds, and the loading arrangement [1]. The cross-section components are split into three categories; flat outstand parts, flat internal parts, and curved internal parts. The width to thickness ratios of each cross-section component is then compared with the slenderness limit for each part. This approach, while simple and easily understood, only accounts for the buckling of each component individually thus ignoring the additional interaction between the individual components [30]. These additional interactions are more likely to occur in complex cross-sections, thus the simplified method and the slenderness limits proposed in EC9 may not be

suitable for the novel optimised section. Additionally, cross-section classification in EC9 assumes a bi-linear elastic perfectly plastic stress-strain model which ignores the advantageous behaviour of aluminium strain hardening [32].

### 5.3 Parametric Study

This section outlines the details and results from the parametric study done to aid with cross-section classification. During the stub column test, the overall buckling mode of the member must be eliminated to ensure failure is only due to local buckling [30]. To prevent overall buckling, BSI [33] recommends the stub column length should be less than 20 times the least cross-section radius of gyration (r). However, to exclude the end effects, Feng and Young [34] noted that the minimum stub column length must be at least three times as long as the greatest cross-section width (B), thus the member length used will be 3B. All the members used have a width and height of 100mm. Consequently, the member length used is 300mm (3B = 300mm).

The section flange and web thicknesses were varied to find out the effectiveness of existing classification techniques on the novel cross-section shapes created. The definitions of flange and web components (parts of section) are shown in Figure 5, and Table 3 outlines the dimensions of flange and web thicknesses used herein.

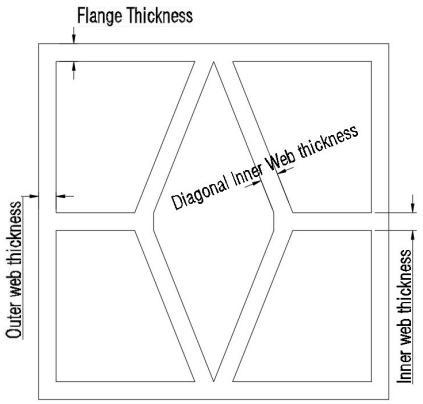


Figure 5: Dimension definitions of cross-section to be investigated

Table 3: List of cross-sections to be used in this study

| Section Number | Flange Thickness (mm) | Web Thickness (mm) | Cross-sectional area ($mm^2$) |
|---|---|---|---|
| 1 | 5 | 5 | 3096 |
| 2 | 5 | 7.5 | 4074 |
| 3 | 5 | 10 | 5005 |
| 4 | 7.5 | 5 | 3502 |
| 5 | 7.5 | 7.5 | 4433 |
| 6 | 7.5 | 10 | 5317 |
| 7 | 10 | 5 | 3908 |
| 8 | 10 | 7.5 | 4792 |
| 9 | 10 | 10 | 1098 |

Each section prepared for this FE study was then classified according to the rules found in EC9. The results of which can be seen in Table 4.

### 5.3.1 Results of parametric study

The FE results are presented as a stress-strain graph in Figure 6 and Figure 7 indicates the typical local buckling failure mode exhibited. Table 4 compares the section classification in EC9 to the class behaviour shown from the FE analyses. The 'FEM class' column was derived from interpreting information from the stress-strain graphs in Figure 6. All the sections are 'Class 1' according to EC9. Of the sections tested, 9 out of 10 have the same 'FEM class' as that from EC9. The only section with a 'FEM class' different to that of EC9 is Section 1 which has the lowest web and flange thicknesses tested in this investigation (see Table 3).

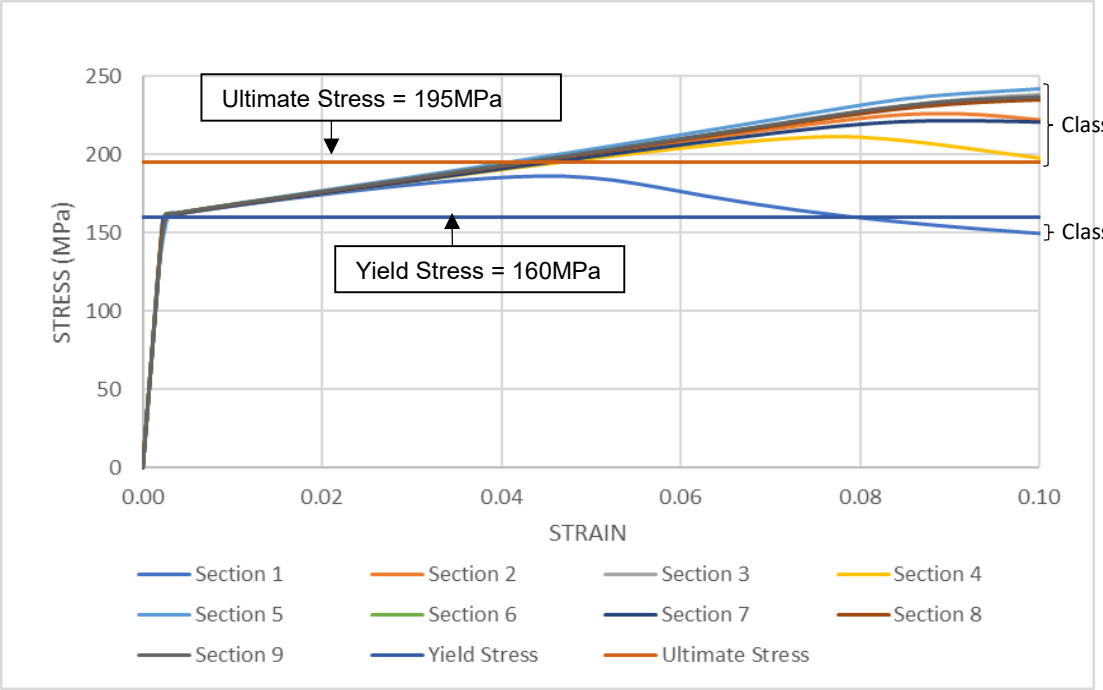


Figure 6: Summary stress-strain diagrams of experimental results

Table 4: Comparison of cross-section classification from FEM results and Eurocode 9

| Section Number | Initial EC9 Class | FEM class |
|---|---|---|
| 1 | Class 1 | Class 3 |
| 2 | Class 1 | Class 1 |
| 3 | Class 1 | Class 1 |
| 4 | Class 1 | Class 1 |
| 5 | Class 1 | Class 1 |
| 6 | Class 1 | Class 1 |
| 7 | Class 1 | Class 1 |
| 8 | Class 1 | Class 1 |
| 9 | Class 1 | Class 1 |

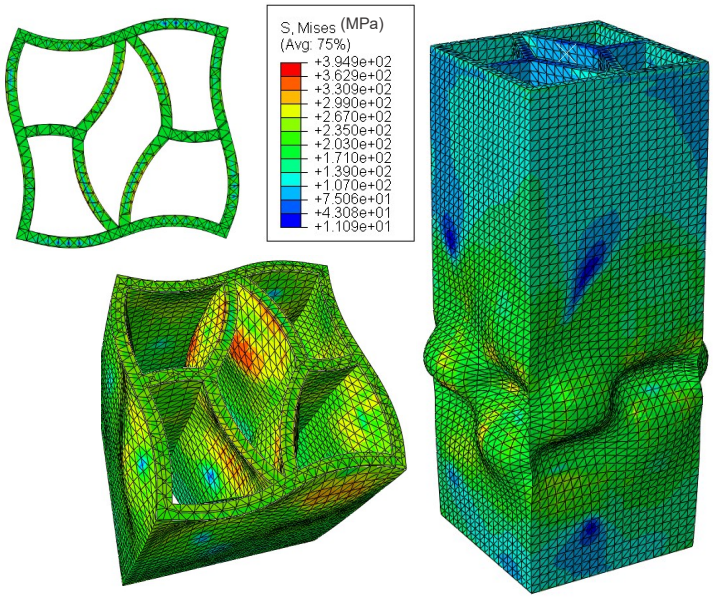


Figure 7: Typical stub-column local buckling failure mode extracted from FEA

## 6 CONCLUDING REMARKS

This paper investigates the performance of previously optimised aluminium profiles [7], designed through advanced structural topology optimisation techniques to develop structurally efficient cross-sections with an improved weight-to-stiffness ratio. A parametric study using FEA was conducted on the optimised sections to aid with the cross-section classification leading to the development of a design approach for optimised profiles [8].

Additional studies were then carried out to improve the fabrication capacity of the novel profile as well as to characterise their compression behaviour. The improvement in their manufacturability was done heuristically by keeping a similar cross-section philosophy whilst providing more uniform cross-section elements with constant thicknesses and curve radii. The most optimum section was chosen after a comparison of the sections under the criteria (i.e., the second moment of area, the radius of gyration, and elastic buckling load).

Stub-column tests were then performed to determine the behaviour of a number of optimised aluminium options under compression and to investigate the effectiveness of using existing classification methods using FEA. It was found that 9 out of 10 of the sections tested behaved as predicted by EC9. A more detailed parametric investigation is required to find out why the classification method found in EC9 did not apply to this optimised shape for thicknesses around 5mm.

Further research will investigate the optimised section resistance under other global and local failure modes such as shear, flexure, and torsion while this study acts as the basis upon which future works on developing sustainable and lightweight structural elements through a combination of design optimisation methodologies can be conducted. Moreover, this study has demonstrated that optimised profiles have the potential to conform and be used along with existing standards.

## REFERENCES


[1] Mazzolani, F.M. 1994. *Aluminium alloy structures*. CRC Press. London.

[2] Chi, Y., Gu, G., Yu, H. and Chen, C. 2018. *Layer surface alloying on aluminium and its alloys: A review*. Optics and Lasers in Engineering. 100, pp.23-37.

[3] Ma, W., Becque, J., Hajirasouliha, I. and Ye, J. 2015. *Cross-sectional Optimisation of cold-formed steel channels to Eurocode 3*. Engineering Structures. 101, pp.641–651.

[4] Anand, K. and Misra, A. (2015). *Topology Optimization and Structural Analysis of Simple Column and Short Pressurized Beams Using Optimality Criterion Approach in ANSYS*. IRJET, 02(3), pp.1408-1415.

[5] Kim, Y. and Kim, T. (2000). *Topology optimization of beam cross sections. International Journal of Solids and Structures*, 37(3), pp.477-493.

[6] Tsavdaridis, K.D. and D'Mello, C. (2012) *Optimisation of Novel Elliptically-Based Web Opening Shapes of Perforated Steel Beams*. Journal of Constructional Steel Research. 76, pp. 39-53.

[7] Grekavicius, L., Hughes, J.A., Tsavdaridis, K.D. and Efthymiou, E. (2016) *Novel Morphologies of Aluminium Cross-Sections Through Structural Topology Optimisation Techniques*. Key Engineering Materials. 710, pp. 321-326.

[8] Tsavdaridis, K.D. Efthymiou, E., Adugu, A., Hughes, J.A., Grekavicius, L., and (2018) *Novel Aluminium Profiles via Structural Topology and Heuristic Optimisation Studies and Cross-Section Classification*. Thin-Walled Structures. 39, pp. 372-388.

[9] Tsavdaridis, K.D., Kingman, J.J. and Toropov, V.V. (2015) *Application of Structural Topology Optimisation to Perforated Steel Beams. Computers and Structures*. 158, pp. 108-123.

[10] Kingman, J.J., Tsavdaridis, K.D., and Toropov, V.V. (2015) *Applications of Topology Optimisation in Structural Engineering: High-rise Buildings & Steel Components*. Jordan Journal of Civil Engineering. 9(3), pp. 335-357

[11] Tsavdaridis, K.D. and D'Mello, C. (2012) *Optimisation of Novel Elliptically-Based Web Opening Shapes of Perforated Steel Beams*. Journal of Constructional Steel Research. 76, pp. 39-53.

[12] Tsavdaridis, K.D., Hughes, J.A., Grekavicius, L. and Efthymiou, E. (2017) *Novel Optimised Structural Aluminium Cross-Sections Towards 3D Printing*. The International Conference on Additive Manufacturing in Products and Applications (AMPA 2017) (ETH) Zürich, Switzerland In: Meboldt M., Klahn C. (eds) Industrializing Additive Manufacturing - Proceedings of Additive Manufacturing in Products and Applications (AMPA 2017). AMPA 2017. Springer, Cham, pp. 34-46.

[13] Burkin, A.R. 1987. *Production of aluminium and alumina, Volume 20*. Chichester: Society of Chemical Industry.

[14] Śliwa, A., Kwaśny, W., Sroka, M. and Dziwis, R. 2017. *Computer simulation of the aluminium extrusion process.* Metalurgija. 56(3–4), pp.422–424.

[15] Gitter, R. 2006. *Aluminium Materials for Structural Engineering – Essential Properties and Selection of Materials*. Structural Engineering International. 16(4), pp.294–300.

[16] Mazzolani, F. 1985. *Aluminium Alloy Structures*. Boston: Pitman.

[17] Mei, Y., Wang, X. and Cheng, G. 2008. *A feature-based topological optimization for structure design*. Advances in Engineering Software. 39(2), pp.71–87.

[18] Eschenauer, H.A. and Olhoff, N. 2001. *Topology optimization of continuum structures: A review*. Applied Mechanics Reviews. 54(4), p.331.

[19] Holmberg, E., Torstenfelt, B. and Klarbring, A. 2013. *Stress constrained topology optimization*. Structural and Multidisciplinary Optimization. 48(1), pp.33–47.

[20] Bendsøe, M.P. 1989. *Optimal shape design as a material distribution problem*. Structural Optimization. 1(4), pp.193–202.
[21] Xie, Y.M. and Steven, G.P. 1993. *A simple evolutionary procedure for structural optimisation*. Computers and Structures. 49, pp.885–896.
[22] Rozvany, G.I.N. 2009. *A critical review of established methods of structural topology optimization*. Structural and Multidisciplinary Optimization. 37(3), pp.217–237.
[23] Ma, W., Becque, J., Hajirasouliha, I. and Ye, J. 2015. *Cross-sectional Optimisation of cold-formed steel channels to Eurocode 3*. Engineering Structures. 101, pp.641–651.
[24] Kim, Y.Y. and Kim, T.S. 2000. *Topology optimization of beam cross sections*. International Journal of Solids and Structures. 37(3), pp.477–493.
[25] Bochenek, B. and Tajs-Zielińska, K. 2015. *Minimal compliance topologies for maximal buckling load of columns*. Structural and Multidisciplinary Optimization. 51(5), pp.1149–1157.
[26] BSI. 2007. *BS EN 1999-1-1:2007. Eurocode 9: Design of aluminium structures - Part 1-1: General structural rules.* United Kingdom: British Standards Institute.
[27] Liu, M., Zhang, L., Wang, P. and Chang, Y. 2015. *Buckling behaviours of section aluminium alloy columns under axial compression*. Engineering Structures. 95, pp.127–137.
[28] Tsavdaridis, K.D. and D'Mello, C. 2011. *FE Modelling Techniques for Web-Post Buckling Response*. 6th European Conference on Steel and Composite Structures, pp.1851–1856.
[29] Mennink, J. 2002. *Cross - sectional stability of aluminium extrusions: Prediction of the actual local buckling behaviour*. PhD thesis. Department of the Built Environment, Eindhoven: Technische Universiteit Eindhoven.
[30] Su, M.N., Young, B. and Gardner, L. 2014. *Testing and Design of Aluminium Alloy Cross Sections in Compression*. Journal of Structural Engineering. ASCE. 140(9).
[31] BSI. 2005. *BS EN 1993-1-1:2005. Eurocode 9: Design of steel structures - Part 1-1: General rules and rules for buildings.* United Kingdom: British Standards Institute.
[32] Su, M.-N., Young, B. and Gardner, L. 2016. *The continuous strength method for the design of aluminium alloy structural elements*. Engineering Structures. 122, pp.338–348.
[33] BSI. 1998. *Structural use of steelwork in building*. United Kingdom: British Standards Institute.
[34] Feng, R. and Young, B. 2015. *Experimental Investigation of Aluminum Alloy Stub Columns with Circular Openings*. American Society of Civil Engineers (ASCE). 141(11), pp.1–10.